OXFORD UNIVERSITY PRESS | Integrative and Comparative Biology

Challenges in modeling pheromone capture by pectinate antennae

Journal:	*Integrative and Comparative Biology*
Manuscript ID	ICB-2020-0039.R1
Manuscript Type:	Symposium article
Date Submitted by the Author:	23-May-2020
Complete List of Authors:	Jaffar Bandjee, Mourad; University of Tours Krijnen, Gijs; University of Twente Faculty of Engineering Technology CASAS, Jerome; Université Francois-Rabelais de Tours, IRBI UMR7261
Keywords:	olfaction, ecomorphology, fluid dynamics, mass transfer, additive printing

Symposium article: Challenges in modeling pheromone capture by pectinate antennae

Mourad Jaffar-Bandjee[1,2], Gijs Krijnen[2], and Jérôme Casas*[1]

[1]Institut de Recherche sur la Biologie de l'Insecte, UMR 7261, CNRS, Université de Tours, France
[2]Robotics and Mechatronics, Technical Medical Centre, University of Twente, the Netherlands

May 28, 2020

Abstract

Insect pectinate antennae are very complex objects and studying how they capture pheromone is a challenging mass transfer problem. A few works have already been dedicated to this issue and we review their strengths and weaknesses. In all cases, a common approach is used: the antenna is split between its macro- and microstructure. Fluid dynamics aspects are solved at the highest level of the whole antenna first, *ie*, the macrostructure. Then, mass transfer is estimated at the scale of a single sensillum, *ie*, the microstructure. Another common characteristic is the modeling of sensilla by cylinders positioned transversal to the flow. Increasing efforts in faithfully modeling the geometry of the pectinate antenna and their orientation to the air flow are required to understand the major advantageous capture properties of these complex organs. Such a model would compare pectinate antennae to cylindrical ones and may help to understand why such forms of antennae evolved so many times among Lepidoptera and other insect orders.

Keywords: olfaction, ecomorphology, fluid dynamics, mass transfer, additive printing

*Corresponding author : jerome.casas@univ-tours.fr

1 Introduction

Insects are highly dependent on olfaction to perform many tasks, such as finding food and locating proper habitats and partners. From this perspective, antennae have a major importance as they are very often the main olfactory organs. Insects display antennae with various shapes [1]. One kind of antennae, the pectinate antennae, has attracted much attention as it is considered to be a very sensitive detector of pheromone in air [2]. The fact that pectinate antennae evolved several times independently in various families of moths [3] and in Coleoptera is also intriguing and a cue that pectinate antennae might have an adaptative advantage over cylindrical ones in certain circumstances. As a consequence, much work has been done to measure how sensitive they are [4, 5, 6, 7], and to understand why they perform so well [8, 9, 10, 11, 12, 13, 14]. Appendages of crustaceans, composed of numerous cylinder-like elements, have also been the objects of many studies and face similar challenges as pectinate antennae in terms of odor capture [15, 16, 17]. Thus, results in crustacean appendages could be used to better understand pectinate antennae and *vice versa* [10].

A major difficulty in the study of pectinate antennae is their complex multi-scale shape. The flagellum, the main branch of the antenna, supports a few dozen rami which are secondary branches. Each ramus bears many hairs, the sensilla, which host the chemical detectors. It should be noted that the whole antenna is usually around a centimeter long whereas the sensilla are only 150 µm long, with a diameter of a few micrometers [2]. Thus, the dimensions of the elements of the antenna spread over four orders of magnitude. On top of that, the shape of the antenna and the relative position of its numerous elements might change with the airflow, adding another layer of complexity.

Because of the complex shape of pectinate antennae, many simplifications have been made on their geometry in the studies dedicated to them. In this work, we firstly present the main challenges faced by any study of pectinate antennae. Secondly, we review the existing works. Finally, we compare them and give some guidelines to develop a model with a faithful geometry which could then be compared with a cylindrical antenna.

2 The problem and its challenges

The capture of pheromone by pectinate antennae is a problem of mass transfer, from the air to the surface of the antennae. The pheromone concentration is usually very low, so the mass transfer equation is the following classical one:

$$\frac{\partial c}{\partial t} + (\vec{v} \cdot \nabla)c = D\nabla^2 c \tag{1}$$

with $\vec{v}$, the velocity of air ($\mathrm{m\,s^{-1}}$)
c, the concentration in pheromone in air ($\mathrm{mol\,m^{-3}}$)
D, the diffusive coefficient of the pheromone in air ($\mathrm{m^2\,s^{-1}}$).

In the mass transfer equation (Equation 1), the air velocity field has a strong influence in the equation and, thus, must be also determined, according to the Naviers-Stokes equations:

$$\nabla \cdot \vec{v} = 0 \tag{2}$$

$$\frac{\partial \vec{v}}{\partial t} + (\vec{v} \cdot \nabla)\vec{v} = -\frac{\nabla P}{\rho} + \nu \nabla^2 \vec{v} \tag{3}$$

with P, the pressure in air ($\mathrm{kg\,m^{-1}\,s^{-2}}$)
ρ, the density of air ($\mathrm{kg\,m^{-3}}$)
ν, the kinematic viscosity of air ($\mathrm{m^2\,s^{-1}}$)

In both cases (Equations 2 and 3), the solutions to the equations depend strongly on the boundary conditions defined by the geometry of the pectinate antenna, by the pheromone concentration at their surface and by the far-field air velocity as the Naviers-Stokes equations are not linear and, thus, must be determined for each air velocity of interest.

The most straightforward method to determine the pheromone capture of an antenna would be to determine the mass flux at the surface of the antenna by solving the Naviers-Stokes and the mass transfer equations. Another solution is to resort to simulations and Computational Fluid Dynamics. Finally, experiments can be done. However, major difficulties prevent an easy identification of the mechanisms of the pheromone capture by pectinate antennae in all these cases. Difficulties arise due to three main reasons (Table 1). Firstly, a pectinate antenna is a very complex geometrical object composed of tens of thousands of sensilla. Secondly, the air flux faced by the moth and, thus, the antennae is not constant. Lastly, the chemical signal is not constant either, due to turbulence in air [18, 19, 20] and often comes in puffs. Pheromone emission it-self is not constant, reinforcing the non-constant nature of the signal [21, 22, 23].

When analytically solving the equations, the complex shape of the pectinate antenna has two implications. Firstly, the boundary conditions are complex to define because the antenna is composed of numerous elements: the flagellum, the rami and the sensilla. Secondly, an antenna covers a wide range of orders of magnitude in terms of dimensions. As a consequence, it is not possible to simplify the Naviers-Stokes equations. For example, in the case of the Stokes regime, the inertial term $(\vec{v} \cdot \nabla)\vec{v}$ (Equation 3) usually drops for slow-moving fluids and small objects. The way of simplifying the Naviers-Stokes equation mainly depends on the Reynolds number Re, which assesses the relative importance of the viscous $\nu \nabla^2 \vec{v}$ and inertial $(\vec{v} \cdot \nabla)\vec{v}$ terms (Equation 3).

In the case of the pectinate antennae, for a characteristic velocity of $0.1\,\mathrm{m\,s^{-1}}$ and a viscosity of air at $15.6 \times 10^{-6}\,\mathrm{m^2\,s^{-1}}$, the characteristic lengths cover a few orders of magnitude: 1 µm for the diameter of the sensilla, to 1 cm for the size of the entire antenna. Thus, the Reynolds numbers are between 0.01 and 100 and it is not possible to make any simplification of the equations by dropping terms for very high and very low Reynolds numbers. The non-constant air flow and concentration conditions imply that the time-depending terms $\frac{\partial c}{\partial t}$ and $\frac{\partial \vec{v}}{\partial t}$ cannot be neglected, neither in the mass transfer equation (Equation 1) nor in the Naviers-Stokes equation (Equation 3), respectively.

The antennal geometry is also a major difficulty for Computational Fluid Dynamics as the tens of thousands of sensilla require the generation of a huge number of elements in the simulation domain. Working on a virtual pectinate antenna would then require much memory storage and computing power. Here again, because of the intermediate Reynolds numbers, it is not possible to simplify the equations. Also, adding a time-dependent component, either through the air flow or through the pheromone concentration, would further increase the complexity of the simulation as well as the computational time.

Experimentation is a good solution to bypass the difficulty of solving, analytically or numerically, the equations. However, the complexity of the shape of the antenna remains a bottleneck. Even though progress has been made, reproducing a pectinate antenna is a difficult task [24] either because of the numerous sensilla to build or because of their tiny dimensions. Sensilla and rami, the main components of the antenna, are elements of high aspect ratios (between 30 and 50) which increases the difficulty to fabricate them even in scaled-up models [25].

Techniques to measure mass transfer are complex. Given the size of a pectinate antenna, any sampling device is expected to have an influence on the air flow, so non-invasive techniques should be preferred. Several techniques exist [26, 27] but, because of the very low concentration in pheromone, Planar Laser-Induced Fluorescence (PLIF) appears to be the most adapted one. This technique consists of using a laser sheet to illuminate the fluid and the molecules of interest. Depending on the intensity of the fluorescent emission, the concentration of the chemical species can be determined. This technique requires that the molecules of the species of interest do fluoresce [28]. If it is not the case, external tracers with good fluorescent properties may be added to the fluid [29, 30]. PLIF has already been used to track odor concentration in air [31]. However, if the diffusive process is not negligible, these tracers should also have the same behavior in air, *i.e.* the same diffusivity. One major advantage of the PLIF technique is that it gives the concentration at any point of the plane illuminated by the laser sheet. However, creating a non-constant flow as well as a non-constant chemical signal can be challenging [31, 29].

Table 1: Three main challenges in dealing with pheromone transport and capture by pectinate antennae and the approaches to overcome them. $\vec{v}$ is the air velocity field and c the pheromone concentration in air.

3 Current models

Due to the challenges faced when studying pectinate antennae, no previously developed model has been able to tackle the entire complexity of the pheromone transfer from the air to the surface of the antenna. Instead, models are usually designed to tackle one aspect of the problems and may mix several approaches in order to compensate the weaknesses of one by the strengths of the other. In the following, we describe the published studies in turn, ordered according to the problems they faced.

3.1 Case 1: an analytical approximation of the mass transfer on a sensillum

In a pioneer work, **Adam and Delbrück [8]** introduced an interesting idea about what they called the reduction of dimensionality. This new idea addressed how the pheromone molecules reach the pores which are small apertures linking the haemolymph inside the sensilla to the exterior environment. They assumed that the pheromone molecules first reach the surface of the sensillum and then diffuse on the 2D surface to the pores. The authors showed that this reduction of dimensionality, from a 3D to a 2D environment, could help to enhance the capture of pheromone by pectinate antennae. However, Futrelle [32] later showed that pheromone rebounding at the surface of the sensillum could also lead to efficient capture of pheromone molecules in the pores. Adam and Delbrück then developed a model of mass transfer of pheromone from the air to the surface of a sensillum modeled as a cylinder. Their approach was reproduced by **Murray [13]** who further extended the analytical calculations. In both cases, the approach is equivalent to split the antenna in several elements and focus on the smallest one. This focus on the smallest element is justified by the fact that the chemical detectors are located within the sensilla. Thus, understanding the mass transfer at the level of the sensilla is an important point. To simplify the problem and make it analytically solvable, the authors of both papers assumed the sensillum to be a cylinder transversal to a steady flow of air. They also assumed a constant pheromone concentration. As a consequence, the terms $\frac{\partial c}{\partial t}$ and $\frac{\partial \vec{v}}{\partial t}$ in equations 1 and 3 drop, respectively. This approach provides two main benefits. The first one is that there is only one cylinder to deal with at a time. The second one is that the transverse cylinder, assumed to be infinite, can be modeled by a 2D circle (Figure 1), thus reducing the complexity of the problem. In such a configuration, the authors were able to analytically solve both the fluid dynamics and mass transfer problems at the finest level of detail. However, one main limitation of this approach is that it does not include the alteration of the flow due to the neighboring

Figure 1: Cylinder modeling a sensillum transversal to the flow and viewed from the top. v_0 is the far-field velocity and c_0 is the far-field concentration. Adapted from [13]

sensilla. In the work of Murray [13], the first coarser level of the antenna takes into account this interaction between the sensilla and is roughly modeled as a multiplying factor of the capture rate of the sensilla. This factor is extrapolated from a study of aerosol capture by closely-packed parallel circular cylinders [33]. The mass transfer is calculated on the second level, which has a very simple shape.

3.2 Case 2: an analytical model of pairs of cylinders

Cheer and Koehl [10], based on [34], also modeled the sensilla as cylinders transversal to the flow. Furthermore, they were also interested in the influence of the rami that support the sensilla and, like the sensilla, modeled them as cylinders transversal to the flow too. The authors looked at a new parameter that could have a major influence on the efficiency of an antenna: the leakiness. Antennae are composed of many elements that generate a resistance to the air flow. Thus, air partly flows through the antenna or around the entire structure. The effect of leakiness may be negligible in the case of highly permeable objects but it has two major consequences on structures with low to medium leakiness. Firstly, the pheromone molecules in the portion of air flowing around the entire structure are not available for capture by the sensilla. Secondly, a low leakiness means a slower air velocity than the far-field one. Indeed, as part of the flow is deflected around the object, the conservation of mass implies that the air going through the object has to flow slower, giving more time to the pheromone molecules to diffuse to the surface of the sensilla. Determining the leakiness of a structure such as a moth antenna is not an easy task: Cheer and Koehl achieved it by solving the velocity profile in two steps. The first step was to determine how air flows between two transversal cylinders (mimicking two rami) at *intermediate* Reynolds number. The mean velocity between the rami was then used as far-field velocity to find the velocity field around two transversal cylinders at *low* Reynolds number (Figure 2 a). Interestingly, the authors had to use two different models of fluid flowing between two cylinders. At the level of the rami, the Reynolds number is high and inertia cannot be neglected. Cheer and Koehl could simplify this inertia term according to the Oseen approximation [35]: the non-linear term $(\vec{v} \cdot \nabla)\vec{v}$ is changed into $(\vec{v}_\infty \cdot \nabla)\vec{v}$. At the level of the sensilla, the Reynolds number drops and the authors used a model that they previously developed for low Reynolds numbers [34]. A major drawback of this analysis is that it deals with the fluid dynamics only and does not determine the pheromone capture by the antenna. This work was extended further by **Schuech *et al* [36]** who ran simulations

Figure 2: Analytical leakiness and simulation mass transfer. a: Varying leakiness between two cylinders. Adapted from [34]. b: Pheromone concentration around a sensillum in an infinite row. Adapted from [36]

to determine the mass capture by an infinite row of cylinders mimicking the sensilla (Figure 2 b). The drawback of considering an infinite array is that it cannot determine the leakiness because the infinity of the array forces the fluid to flow entirely between the cylinders. By contrast, the benefit of such a model is that it is convenient to run simulations on: in an infinite array of evenly-spaced cylinders, only one cylinder with periodic boundary conditions is sufficient to determine the behavior of the entire array.

3.3 Case 3: Puffs of odors and temporal patterns of the pheromone signal

To avoid the complexity of analytically calculating the leakiness of the antenna, **Humphrey and Haj-Hariri [11]** split the antenna in three levels and modeled the first one as a permeable cylinder (Figure 3) with a given leakiness (equal to 5 and 10%). Using approximations, they determined the flow profile around the permeable cylinder as well as the mass transport of pheromone at the entrance of the cylinder. Inside the permeable cylinder, there are sensilla but there is no space dependence anymore. The concentrations are uniform and a mass balance determines the concentration of pheromone in the air inside the antenna and on the surface of the sensilla. The concentration at the surface of the pores (located on the surface of the sensilla) is considered to be equal to the concentration at the surface of the sensilla. The depletion of pheromones, due to the pheromone molecules entering into the tubule, is considered to be negligible. Eventually, the pheromone molecules enter the tubules through the pores and migrate to the end of the tubules where they are detected. This model is interesting because it gives a system of analytical equations and a numerical solution to temporal chemical variations and tackles the mass transfer problem at the two levels of the antenna. However, since we were not able to find sufficient boundary values in [11] we could not solve their system of equations. their calculations (See Supplementary materials). However, the leakiness is a fixed parameter that is independent of the air velocity. Experiments conducted by Vogel [14], and very recently confirmed by us [37], showed that the leakiness does actually depend on air velocity, as expected because of the dependence of the boundary layer thickness on velocity. It has also been shown in crustacean and copepod appendages that leakiness varies with water velocity [38] and that the change of regime from highly leaky to almost impermeable can be used to improve the performance of the appendages [15, 39].

Figure 3: Permeable cylinder and mass transfer inside the antenna. $\vec{v_0}$ and c_0 are respectively the velocity and far-field concentration at the entrance of the antenna. c_1 is the concentration inside the antenna and c_S is the concentration at the surface of the sensilla. q_{in} is the mass flux entering the permeable cylinder modeling the antenna. q_{ads} and q_{des} are the mass flux that are respectively adsorped and desorped at the surface of the sensilla. q_{dif} is the mass flux entering the tubule and q_{out} is the mass flux going out of the antenna. Adapted from [11].

Figure 4: Experimental leakiness and simulated mass capture. a: Experimental set-up to measure the periodic air flow. b: Simulation to determine the random walk of a pheromone molecule. Reproduced from [12].

3.4 Case 4: mixing experiments, analytical modeling and simulations

Moths perform active sensing, called sniffing, by beating their wings to generate a flow of air through their antennae. Wing beating is periodic and is thus expected to create periodic air flows. To our knowledge, **Loudon and Koehl [12]** are the first ones to measure such flows and to use them in a model of pectinate antennae. This work is an original combination of experiment, analytical modeling and simulation. They took an experimental approach to measure the periodic air flow with a hot wire anemometer (Figure 4a). However, they used the mean flow as input of the model of Cheer and Koehl [10] to determine the leakiness. Thus, even though they measured periodic air flow, their work is based on a constant air flow model. They then conducted random-walk simulations using the air velocity profile they measured to determine how many molecules would reach the surface of the sensilla (Figure 4b).

3.5 Case 5: the complementary case of a terrestrial crustacean

Crustaceans, related to the Insects among the Arthropods [40], have appendages to smell odors. Even though the geometries of such appendages are different from the one of the pectinate antenna, the techniques used to determine the mass transfer are similar and should also be considered. We report here a study of the appendage of a terrestrial crustacean, *Coenobita rugosus* [41]. This crustacean capture odors in air and the physics of such a phenomenon are the same as the one of the pectinate antenna. This study is divided in two parts. Firstly, the authors measured experimentally the leakiness of the appendage. Secondly, they ran simulations to determine the mass capture by the appendage. **Waldrop and Koehl [41]** resorted to Particle Image Velocimetry (PIV) to measure the leakiness. This technique consists of seeding a fluid with particles and illuminate

them with a laser sheet. By following the displacement of the particles, it is possible to calculate the velocity field of the fluid. However, crustacean appendages are very small and move very fast, so, in their experiments, the authors used dynamic scaling to enhance the size of their artificial appendage and decrease the velocity. Dynamic scaling relies on keeping the Reynolds number constant. The authors then ran Monte Carlo simulations to determine the odor transport to the appendages. A similar approach, mixing PIV measurements and simulations, has been done on aquatic crustaceans [16].

Table 2: Comparison of the models of pheromone capture by pectinate antennae (and terrestrial crustacean appendage, Case 5).

4 Discussion

4.1 Comparison of the models

Given the complexity of the antenna, all these previous studies had to give up on some aspects to gain on other ones (Table 2). For example, Murray [13] could completely define the fluid dynamics and mass transfer around sensilla analytically. However, his model was developed for the case of a steady state flow and he did not calculate the leakiness of the antenna, which is an important parameter. Cheer and Koehl [10] focused on determining the leakiness but, in order to keep calculations doable, had to consider two sensilla only and not a row of them. They also did not look into the mass transfer problem. Humphrey and Haj-Hariri [11] could investigate the temporal pattern of a chemical signal reaching the antenna. However, their estimated leakiness was a fixed parameter independent of the velocity. They also greatly simplified the geometry of the antenna by modeling the array of sensilla and rami by a permeable cylinder. Loudon and Koehl [12] measured the non-constant air flow facing the antennae on a real moth but calculated the leakiness in a constant air flow case and simulated the random walk of pheromone molecules. They could not determine the temporal pattern of the chemical signal in contrast to Humphrey and Haj-Hariri [11]. Waldrop and Koehl [41] resorted to PIV to measure the velocity field in a steady-state regime and simulations to determine the mass capture. Thanks to simulations, they had access to the temporal pattern of the flux of odor on the appendage of the hermit crab. However, the geometry of such an appendage is much simpler than the one of a pectinate antenna. In conclusion, a single model can hardly be expected to capture the functioning of a multiscale antenna in its entire nature; one must choose which aspects to focus on.

Useful information can be extracted from our review to design a model with a more faithful geometry. In fact, there is a common approach to all of them. The mass flux on the sensilla is the main quantity of interest. Given the complexity of its geometry, an antenna is usually divided in two levels, which we call the macrostructure and the microstructure. The microstructure encompasses the sensilla which host the chemical detectors and, thus, both the fluid dynamics and the mass transfer need to be determined at this level. Thanks to the small size of sensilla, the assumption of Stokes flow can be used at this level. The microstructure is modeled in varying ways depending on whether the objective is to determine the fluid dynamics, the leakiness or the mass transfer at the surface of the sensilla. Indeed, in the case of leakiness, the finite nature of the antenna is important as it is leakiness which expresses what goes around and what goes through the antenna. Regarding mass transfer, the interesting point is the mass capture of an average sensillum. A model with an infinite number of cylinders is then more interesting since, with appropriate boundary conditions, it allows to reduce the study to a single sensillum. Once the physics at the microstructure level is understood, it is then possible to simplify the macrostructure. The macrostructure determines the airflow faced by the microstructure and, thus, only fluid dynamics are considered. Both leakiness and mass transfer by diffusion are important phenomena in air [42]. So, none can be neglected as in the case of marine crustaceans [15].

4.2 Understanding the geometry of pectinate antennae

All models described in the previous sections attempted a better understanding of the particular ability of pectinate antennae at detecting low concentrations of pheromone in air. However, a recent study on filiform antennae [43] has shown that small details such as scales can have an important influence on the olfactory performance. Even though pectinate antennae do not have scales on their rami [9, 44, 37], it is still important to faithfully model them. One weakness of the models we reviewed is the orientation of the rami and sensilla which are assumed to be transversal to the air flow. It has indeed been shown that the orientation of the rami does have an influence on the pheromone capture [45]. We expect the orientation of the sensilla to have an effect as it has been shown that the sensilla may be longitudinal to the flow [9, 46]. For the purpose of designing a new model with a more faithful geometry of the pectinate antenna, special care should be given to the determination of mass transfer at the sensillum level and, especially, leakiness. Indeed, leakiness determines the portion of air going through the antenna but, also,

the average air velocity within the antenna. A highly-leaky antenna allows much air to flow through it but is expected to capture little of its pheromone whereas a poorly-leaky one allows little air but most of its pheromone should reach its surface. Thus, a model without a good assessment of leakiness cannot be accurate so it may be helpful to look at previous works which have attempted to measure it on pectinate antennae. Vogel [14] and Loudon and Davis [47] used dyes to visualize the flow through and around pectinate antennae. Particle Image Velocimetry, the technique used by Waldrop and Koehl [41] for crustacean appendages, could also help to accurately measure the leakiness of antennae. It should also be noted that Vogel [14] showed that the leakiness varies with the air velocity, so determining the leakiness on a wide range of air velocities encountered by the moth will be necessary. Regarding mass transfer on sensilla, a model with longitudinal cylinders might be more appropriate than one with transversal cylinders.

Pectinate antennae have gathered sustained interest because they are thought to have better performance at detecting low concentrations of pheromone in air than antennae with different shapes. The most straightforward solution to this question is to determine the optimal shape among all the possible shapes of antennae. However, finding such an optimum is a very complex task. Comparison with other existing shapes of antennae would also be informative and a much easier problem. For example, lamellate antennae of beetles are also considered to be effective at detecting low-concentrated odors in air [48]. Comparison with cylindrical antennae would also be very useful. Indeed, cylindrical antennae are the basal shapes from which pectinate antennae evolved at least 17 times independently [3]. Thus, the specific shape of pectinate antennae should have an impact on their ability to detect pheromone and should be modeled differently from the cylindrical antenna. A closer look at the geometries used in the previous models shows that Case 1, focusing on the sensillum level, should also be valid for cylindrical antenna and, thus, cannot explain the particular performance of pectinate ones. The model of porous cylinder in Case 3 is also very close to a cylinder. Cases 2 and 4, both based on [10], model two rami. In this way, they take into account the interaction of the rami and, thus, are more realistic models. However, pectinate antennae have a few dozen rami [49] so these models are still far remotely modeling a pectinate antenna. We still lack proper templates of models of cylindrical and pectinate antennae to do meaningful comparisons. Pursuing the development of more realistic models is therefore a high priority if one ought to assess the alleged improved pheromone capture by pectinate antennae. In the meantime, it would be interesting to investigate other shapes of antennae in order to better

Figure S 1: Permeable cylinder and mass transfer inside the antenna. $\vec{v_0}$ and c_0 are respectively the velocity and far-field concentration at the entrance of the antenna. c_1 is the concentration inside the antenne and c_S is the concentration at the surface of the sensilla. q_{in} is the mass flux entering the permeable cylinder modeling the antenna. q_{ads} and q_{des} are the mass flux that are respectively adsorped and desorped at the surface of the sensilla. q_{dif} is the mass flux entering the tubule and q_{out} is the mass flux going out of the antenna. Adapted from [11].

understand why they are so diverse [50]. The approach used so far, *i.e,* determining leakiness of entire antennae and mass transfer at the sensillum scale, can be applied to a wider range of antennal shape, from lamellate to plumose, thereby putting the ecomorphology of arthropod antennae within the realm of olfaction.

5 Supplementary materials: the system of equations of Humphrey and Haj-Hariri [11]

Humphrey and Haj-Hariri were interested in calculating the temporal pattern of the chemical signal detected by a moth. They modeled a pectinate antenna with a permeable cylinder. Once the air is inside the antenna, a mass balance is made to determine what goes out of the antenna, what is adsorped on and what is desorped from the sensilla. Then, a portion of the pheromone stuck at the surface of the sensilla enters into a tubule and pheromone diffuses to the end of the tubule where the chemical detectors are located.

Using an approximation of Hiemenz flow, the authors determined the fluid dynamics upstream of the antenna. They assumed that the horizontal component of the flow had the following expression (see Table S 1):

$$u = \frac{2v^*}{a} f'(\eta) x$$

with f an unknown function.

They then obtained Equation S1 (Table S 2).

The expression of u, the horizontal component of the flow, was also used in the mass transport equation which was adimensionalized to obtain Equation S2 (Table S 2).

Equation S3 (Table S 2) was obtained by doing a mass balance on the inside of the cylinder modeling the antenna. Pheromone comes in from the air flowing inside the antenna and is modeled by a flux q_{in}. Pheromone is then adsorped on the surface of the sensilla at a rate q_{ads} and desorp at a rate d_{des}. Eventually, air goes out of the antenna and carries along a flux of pheromone q_{out}. Mass balance gives:

$$q_{\text{in}} = q_{\text{out}} + (q_{\text{ads}} - q_{\text{des}})\frac{A_{ST}}{A_A}$$

To obtain Equation S3, we replace each term by their following expression:

$$q_{\text{in}} = \left(v_0 c_0(t) + D\frac{\partial c_0(t)}{\partial y}\right)$$

$$q_{\text{out}} = v_0 c_I(t)$$

$$q_{\text{ads}} = k_1\left(c_{\text{Smax}} - c_{\text{S}}(t)\right)\left(c_{\text{I}}(t) - k_2 c_{\text{S}}(t)\right)$$

$$q_{\text{des}} = k_3 c_{\text{S}}(t)$$

The authors then made a mass balance on the surfaces of the sensilla and obtained the following equation:

$$\frac{\mathrm{d}c_{\text{S}}(t)}{\mathrm{d}t} = (q_{\text{ads}} - q_{\text{des}}) - d_{\text{dif}}\frac{A_{PT}}{A_A}$$

Because $\frac{A_{PT}}{A_A} \approx 0.001$, the term $d_{\text{dif}}\frac{A_{PT}}{A_A}$ can be neglected and the author obtained the Equation S4.

Equation S5 is the 1D equation of diffusion of the pheromone in the tubule.

All the equations are summarized in Table S 2. The system is composed of five equations and five unknown variables, f, C, c_I, c_S and c. However, Equation S2 has only one boundary condition in $y \to \infty$. Equation S3 is considered, according to the authors, as the boundary condition of Equation S2 for $y = 0$. The problem is that one has, then, only four equations for 5 unknown variables. Since we were not able to find sufficient boundary values in [11] we could not solve their system of equations.

Table S 1: Variables used in the model of Humphrey and Haj-Hariri

Table S 2: System of equations

References

[1] C. Loudon, Antennae. In *Encyclopaedia of Insects*, (V.H. Resh and R.T. Cardé, editors), ch. 6, pp. 21-23, Amsterdam, London: Academic Press, 2009

[2] K.-E. Kaissling, Pheromone Reception in Insects: the example of silk moths. In *Neurobiology of chemical communication*, (C. Mucignat-Caretta, editor), ch. 4, pp. 99-146, Boca Raton: CRC Press/Taylor & Francis, 2014

[3] M.R.E. Symonds, T.L. Johnson and M.A. Elgar, Pheromone production, male abundance, body size, and the evolution of elaborate antennae in moths. *Ecology and Evolution* vol. 2, no. 1, pp. 227-246, 2011.

[4] J. Boeckh, K.-E. Kaissling and D. Schneider, Insect olfactory receptors. In *Cold Spring Harbor symposia on quantitative biology*, vol. 30, pp. 263-280, Cold Spring Harbor Laboratory Press, 1965.

[5] K.-E. Kaissling, The sensivity of the insect nose: the example of *Bombyx mori*. In *Biologically Inspired Signal Processing for Chemical Sensing*, (A. Gutiérrez and S. Marco, editors), ch. 3, pp. 45-52, Berlin, Heidelberg: Springer, 2009.

[6] K.-E. Kaissling, E. Priesner, Die Riechschwelle des Seidenspinners. *Naturwissenschaften*, vol. 57, no. 1, pp. 23-28, 1970.

[7] D. Schneider, Electrophysiological investigation on the olfactory specificity of sexual attracting substances in different species of moths. *Journal of Insect Physiology*, vol. 8, no. 1, pp. 15-30, 1962.

[8] G. Adam and M. Delbrück, Reduction of dimensionality in biological diffusion processes. In *Structural chemistry and molecular biology*, (A. Rich, N.R. Davidson and L. Pauling, editors), pp. 198-215, San Francisco: WH Freeman, 1968.

[9] J. Boeckh, K.-E. Kaissling and D. Schneider, Sensillen und Bau der Antennengeißel von *Telea polyphemus*. *Zoologische Jahrbücher/Abteilung für Anatomie und Ontogenie der Tiere*, vol. 78, pp. 559-584, 1960.

[10] A.Y.L. Cheer and M.A.R. Koehl, Fluid flow through filtering appendages of insects. *Journal of Mathematics Applied in Medicine and Biology*, vol. 4, no. 3, pp. 185-199, 1987.

[11] J.A.C. Humphrey and H. Haj-Hariri, Stagnation point flow analysis of odorant detection by permeable moth antennae. In *Frontiers in Sensing*, (F.G. Barth, J.A.C. Humphrey and M.V. Srinivasan, editors), pp. 171-192, Vienna: Springer, 2012.

[12] C. Loudon and M.A.R. Koehl, Sniffing by a silkworm moth: wing fanning enhances air penetration through and pheromone interception by antennae. *Journal of Experimental Biology*, vol. 203, no. 19, pp. 2977-2990, 2000.

[13] J.D. Murray, Reduction of dimensionability in diffusion processes: antenna receptors of moths. In *Nonlinear Differential Equation Models in Biology*, pp. 83-127, Oxford: Oxford University Press, 1977

[14] S. Vogel, How much air passes through a silkmoth's antenna? *Journal of Insect Physiology*, vol. 29, no. 7, pp. 597-602, 1983.

[15] J.A. Goldman and M.A.R. Koehl, Fluid Dynamic Design of Lobster Olfactory Organs: High Speed Kinematic Analysis of Antennule Flicking by *Panulirus argus*. *Chemical Senses*, vol. 26, no. 4, pp. 385-398, 2001.

[16] M.T. Stacey, K.S. Mead and M.A.R. Koehl, Molecule capture by olfactory antennules: Mantis shrimp. *Journal of Mathematical Biology*, vol. 44, no. 1, pp. 1-30, 2002.

[17] M.A. Reidenbach and M.A.R. Koehl, The spatial and temporal patterns of odors sampled by lobsters and crabs in a turbulent plume. *Journal of Experimental Biology*, vol. 214, no. 18, pp. 3138-3153 2011.

[18] J. Murlis, J.S. Elkinton and R.T. Cardé, Odor Plumes And How Insects Use Them. *Annual Review of Entomology*, vol. 37, no. 1, pp. 505-532, 1992.

[19] A. Celani, E. Villermaux and M. Vergassola, Odor landscapes in turbulent environments. *Physical Review X*, vol. 4, no. 4, pp. 1-17, 2014.

[20] L. Conchou, P. Lucas, C. Meslin, M. Proffit, M. Staudt and M. Renou, Insect Odorscapes: From Plant Volatiles to Natural Olfactory Scenes. *Frontiers in Physiology*, vol. 10, 2019.

[21] W.E. Conner, R.P. Webster and H. Itagaki, Calling behaviour in arctiid moths: the effects of temperature and wind speed on the rhythmic exposure of the sex attractant gland. *Journal of Insect Physiology*, vol. 31, no. 10, pp. 815-820, 1985.

[22] S.P. Foster, K.G. Anderson and J. Casas, Calling behavior and sex pheromone release and storage in the moth *Chloridae virescens*. *Journal of Chemical Ecology*, vol. 46, no. 1, pp. 10-20, 2020.

[23] C. Schal and R.T. Cardé, Rhythmic extrusion of pheromone gland elevates pheromone release rate. *Experientia*, vol. 41, pp. 1617-1619, 1985.

[24] T.L. Spencer, N. Lavrik and D.L. Hu, Synthetic moth antennae fabricated as preconcentrator for odor collection. In *ISOEN 2017 - ISOCS/IEEE International Symposium on Olfaction and Electronic Nose*, pp. 1-3, 2017.

[25] M. Jaffar-Bandjee, J. Casas and G.J.M. Krijnen, Additive manufacturing: state of the art and potential for insect science. *Current Opinion in Insect Science*, vol. 30, pp. 79-85, 2018.

[26] U. Timm, E. Lewis, D. McGrath, J. Kraitl and H. Ewald, LED based sensor system for non-invasive measurement of the hemoglobin concentration in human blood. In *13th International Conference on Biomedical Engineering*, pp. 825-828, Berlin, Heidelberg: Springer, 2009.

[27] M. Hofmann, G. Fischer, R. Weigel and D. Kissinger, Microwave-based noninvasive concentration measurements for biomedical applications. *IEEE Transactions on microwave theory and techniques*, vol. 61, no. 5, pp. 2195-2204, 2013.

[28] R. Bazile and D. Stepowski, Measurements of vaporized and liquid fuel concentration fields in a burning spray jet of acetone using planar laser induced fluorescence. *Experiments in Fluids*, vol. 20, no. 1, pp. 1-9, 1995.

[29] J.P. Crimaldi, Planar laser induced fluorescence in aqueous flows. *Experiments in Fluids*, vol. 44, no. 6, pp. 851-863, 2008.

[30] I. van Cruyningen, A. Lozano and R.K. Hanson, Quantitative imaging of concentration by planar laser-induced fluorescence. *Experiments in Fluids*, vol. 10, no. 1, pp. 41-49, 1990.

[31] E.G. Connor, M.K. McHugh and J.P. Crimaldi, Quantification of airborne odor plumes using planar laser-induced fluorescence. *Experiments in Fluids*, vol. 59, no. 9, pp. 1-11, 2018.

[32] R.P. Futrelle, How molecules get to their detectors: the physics of diffusion of insect pheromones. *Trends in Neurosciences*, vol. 7, no. 4, pp. 116-120, 1984.

[33] N.A. Fuchs and I.B. Stechkina, A note on the theory of fibrous aerosol filters. *Annals of Occupational Hygiene*, vol. 6, no. 1, pp. 27-30, 1963.

[34] A.Y.L. Cheer and M.A.R. Koehl, Paddles and rakes: Fluid flow through bristled appendages of small organisms. *Journal of Theoretical Biology*, vol. 129, no. 1, pp. 17-39, 1987.

[35] C.W. Oseen, Über die Stokes' sche Formel und über eine verwandte Aufgabe in der Hydrodynamik. *Arkiv för Matematik, Astronomi och Fysik*, vol. 6, p. 1, 1910.

[36] R.C. Schuech, M.T. Stacey, M.F. Barad and M.A.R. Koehl, Numerical simulations of odorant detection by biologically inspired sensor arrays. *Bioinspiration and Biomimetics*, vol. 7, no. 1, 2012.

[37] M. Jaffar-Bandjee, T. Steinmann, G.J.M. Krijnen and J. Casas, Leakiness and flow capture ratio of insect pectinate antennae. *Journal of the Royal Society Interface - In press*, 2020.

[38] M.A.R. Koehl, Biomechanics of microscopic appendages: functional shifts caused by changes in speed. *Journal of Biomechanics*, vol. 37, no. 6, pp. 789-795, 2004.

[39] M.A. Reidenbach, N. George and M.A.R. Koehl, Antennule morphology and flicking kinematics facilitate odor sampling by the spiny lobster, *Panulirus argus*. *Journal of Experimental Biology*, vol. 211, no. 17, pp. 2849-2858, 2008.

[40] G. Giribet and G.D. Edgecombe, The Phylogeny and Evolutionary History of Arthropods. *Current Biology*, vol. 29, no. 12, pp. R592-R602, 2019.

[41] L.D. Waldrop and M.A.R. Koehl, Do terrestrial hermit crabs sniff? Air flow and odorant capture by flicking antennules. *Journal of the Royal Society, Interface*, vol. 13, no. 114, p. 20150850, 2016.

[42] L.D. Waldrop, Y. He and S. Khatri, What Can Computational Modeling Tell Us about the Diversity of Odor-Capture Structures in the Pancrustacea? *Journal of Chemical Ecology*, vol. 44, no. 12, pp. 1084-1100, 2018.

[43] Q. Wang, Y. Shang, D.S. Hilton, K. Inthavong, D. Zhang and M.A. Elgar, Antennal scales improve signal detection efficiency in moths. *Proceedings of the Royal Society B*, vol. 285, no. 1874, p. 20172832. 2018.

[44] K.-E. Kaissling, Sensory transduction in insect olfactory receptors. In *Biochemistry of sensory functions*, (L.Jaenicke, editor), pp. 243-273, Berlin, Heidelberg: Springer, 1974.

[45] T.L. Spencer, N. Mohebbi, G. Jin, M.L. Forister, A. Alexeev and D.L. Hu, Moth-inspired methods for particle capture on a cylinder. *Journal of Fluid Mechanics*, vol. 884, p. A34, 2020.

[46] D. Schneider and K.-E. Kaissling, Der Bau der Antenne des Seidenspinners Bombyx mori L. III. Das Bindegewebe und das Blutgefäß. *Zoologische Jahrbücher/Abteilung für Anatomie und Ontogenie der Tiere*, vol. 77, pp. 111-132, 1959.

[47] C. Loudon and E.C. Davis, Divergence of streamlines approaching a pectinate insect antenna: Consequences for chemoreception. *Journal of Chemical Ecology*, vol. 31, no. 1, pp. 1-13, 2005.

[48] A. Ramsey, T.F. Houston, A.D. Ball, T. Goral, M.V.L. Barclay and J.P.L. Cox, Towards an Understanding of Molecule Capture by the Antennae of Male Beetles Belonging to the Genus Rhipicera (Coleoptera, Rhipiceridae). *The Anatomical Record*. vol. 298, no. 9, pp. 1519-1534, 2015.

[49] R. Rougerie, Phylogénie et biogéographie des Saturniinae (Lepidoptera: Bombycoidea, Saturniidae): Approche morphologique

et moléculaire. PhD thesis, Muséum National d'Histoire Naturelle, 2005.

[50] M.A. Elgar, D. Zhang, Q. Wang, B. Wittwer, H.T. Pham, T.L. Johnson, C.B. Freelance and M. Coquilleau, Insect Antennal Morphology : The Evolution of Diverse Solutions to Odorant Perception. *Yale Journal of Biology and Medecine*, vol. 91, no. 4, pp. 457-469, 2018.

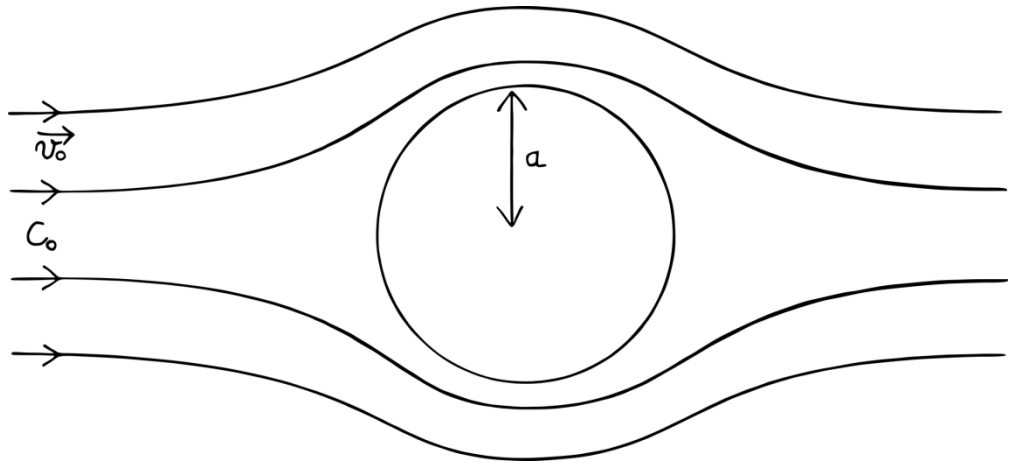

181x82mm (300 x 300 DPI)

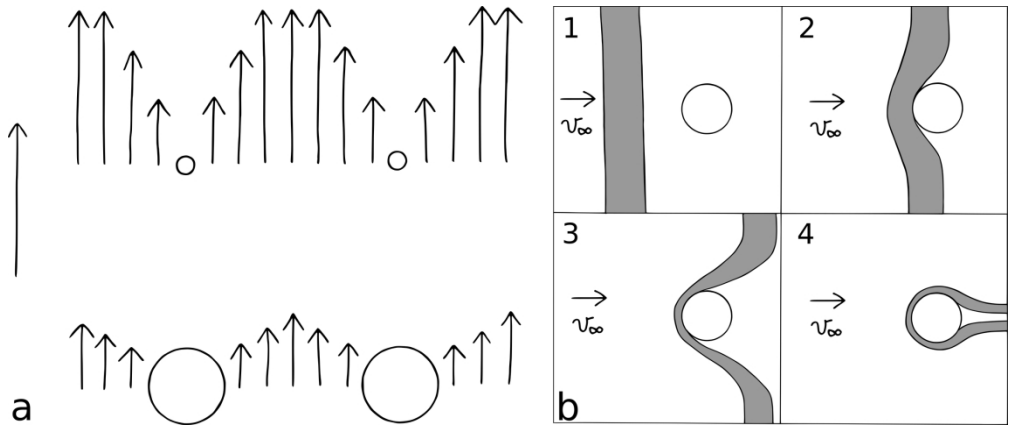

223x93mm (300 x 300 DPI)

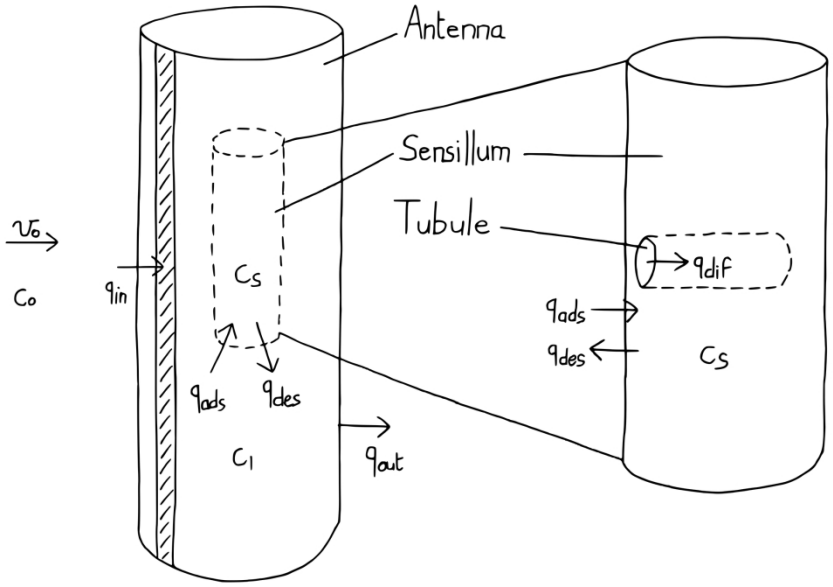

225x170mm (300 x 300 DPI)

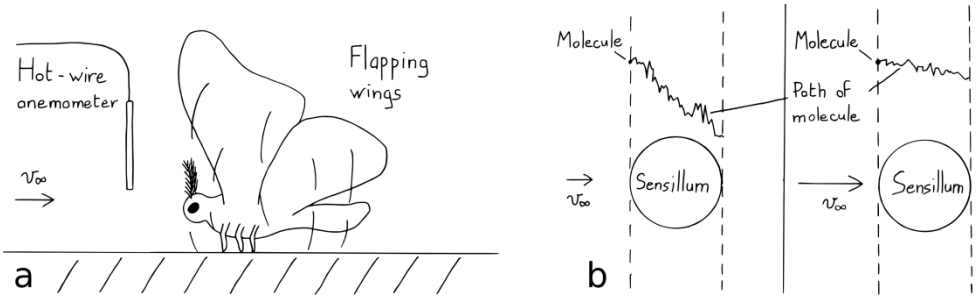

326x95mm (300 x 300 DPI)

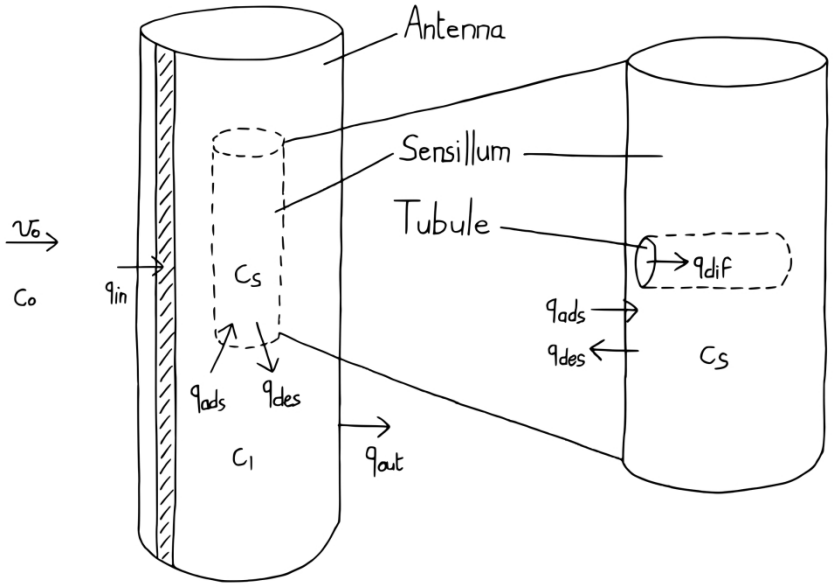

225x170mm (300 x 300 DPI)

	Problems			
Solutions		Complex geometry	Non-constant airflow	Non-constant concentration
	Analytical solution	Complex boundary conditions	Time and spatial dependence of v	Time and spatial dependence of *c*
	Simultaions	Huge number of elements	Time and spatial dependence of v	Time and spatial dependence of *c*
	Experiment	Difficulty to build artificial antennae	Generation of a complex flow	Generation of odor puffs

	Case 1 [13]	Case 2 [10,36]
Objective	Reduction of dimensionality may explain the efficiency of pectinate antennae	Development of a model to predict the leakiness of small animal structures and temporal pattern of the chemical signal
Geometry of the antenna for the fluid dynamics	Collections of sensilla modeled by cylinders. A multiplying factor of capture accounts for the interaction between sensilla.	The rami are modeled by two cylinders which determine the incoming flow on the sensilla modeled by two smaller cylinders, all transversal to the flow.
Calculation of the air flow	Steady-state Stokes flow around each sensillum at air velocity of 1 m/s	Steady-state Oseen flow around the rami and Stokes flow around the sensilla at air velocities of 0.75 and 1 m/s
Geometry of the antenna for mass transfer	Single sensillum modeled	Infinite row of sensilla modeled as cylinders transversal to the flow
Mass transfer	Steady-state transport equation	Transport equation and pulse of pheromone
Variable that measures the efficiency of the antenna	Flux of pheromone	Leakiness and temporal pattern of the pheromone flux on the sensilla
Solving method	Analytical approximations of some physical quantities	Analytical solutions with numerical resolution for the air dynamics and numerical resolution for the mass transfer

Case 3 [11}	Case 4 [12]	Case 5 [41]
Better understanding of the physics involved in olfaction of pectinate antennae	Effect of sniffing on pheromone capture	The evolution of crustaceans olfactory appendages from a marine lifestyle to a terrestrial one
The antenna is modeled as an infinite cylinder transversal to the flow and with a coefficient of permeability.	The incoming air velocity is measured on a real antenna and the leakiness is determined with the same method as in Model 2.	The appendage of a hermit crab is reproduced with a scaling factor. It is a cylinder transversal to the flow with smaller ones beside it.
Steady-state Stokes flow around the antenna at air velocities of 0.5 and 1 m/s	Steady-state Oseen flow around the rami and Stokes flow around the sensilla at air velocity of 0.35m/s	PIV measurements at two velocities at water velocities of 0.061 and 0.11 m/s
Uniform concentration inside the antenna and 1D diffusion in the sensilla	Sensilla modeled as cylinders transversal to the flow	Cylinders transversal to the flow
Mass balance and transport equation on a pulse of pheromone	Probability of molecule interception	Uniform initial concentration but temporal pattern of capture
Time detection of the peak of concentration of pheromone	Flux of pheromone	Flux of pheromone depending on time
Numerical resolution of a system of partial differential equations	Experimental measure of the incoming air flow, analytical solutions with numerical resolution for the air dynamics and random-walk simulations for the mass transfer	Experimental measure of the air velocity field and random-walk simulations for the mass transfer

Symbol	Parameter	Unit
ν_f	Kinematic viscosity of air	m^2s^{-1}
α	Antenna radius	m
v_∞	Far-field fluid velocity	m s^{-1}
$v^* = v_\infty - v_0$		m s^{-1}
u	Horizontal velocity	m s^{-1}
δ	Boundary layer thickness	m
$\eta = \frac{y}{\delta}$	Adimensionalized y-coordinate	Adimensional
$\Phi = \frac{v_0}{v_\infty}$	Antenna permeability	Adimensional
$\mathrm{Re}_\infty = \frac{dv_\infty}{\nu_f}$	Antenna Reynolds number	Adimensional
D	Diffusive coefficient of the pheromone in air	m^2s^{-1}
D_t	Diffusive coefficient of the pheromone in the tubule	m^2s^{-1}
$c_{S\max}$	Maximum concentration of pheromone on the sensillum surface	g m^{-2}
L_t	Length of the tubule	m
A_A	Surface of the antenna	m^2
A_{ST}	Surface of the sensilla	m^2
A_{PT}	Surface of the pores	m^2
T_P	Pheromone pulse time	s
k_1	Sensillum adsorption constant	$m^3g^{-1}s^{-1}$
k_2	Air-to-sensillum surface concentration equilibrium constant	m^{-1}
k_3	Sensillum desorption constant	s^{-1}
k_4	Outer-to-inner sensillum surface concentration equilibrium constant	m^{-1}

	Equation	
Equation S1	$f'^2 - \left(f + \frac{\Phi}{2}\sqrt{\mathrm{Re_d}}\right)f'' = 1 + (1+\Phi)f'''$	Velocity field
	$f(0) = 0, f'(0) = 0, f'(\eta \to \infty) = 1$	Boundary conditions
Equation S2	$\frac{\partial C}{\partial \tau} - \left[f + \frac{\Phi}{2}\sqrt{\mathrm{Re_d}}\right]\frac{\partial C}{\partial \eta} = \frac{1}{Sc}\frac{\partial^2 C}{\partial \eta^2}$	Concentration field upstream of the antenna
	$C(y \to \infty, t) = C_\infty(t) = \frac{1}{2}(1 - \cos\frac{2\pi t}{T_\mathrm{P}})$	Far-field boundary condition
Equation S3	$v_0 c_0(t) + D\frac{\partial c_0}{\partial y}(t) = v_0 c_I(t) + [k_1(c_{s\max} - c_S(t))(c_I(t) - k_2 c_S(t)) - k_3 c_S(t)]\frac{A_\mathrm{ST}}{A_\mathrm{A}}$	Mass balance on control Volume 1
Equation S4	$\frac{dc_S(t)}{dt} = \frac{k_1(c_{s\max} - c_S(t))(v_0 c_0(t) + D\frac{\partial c_0}{\partial y}(t) + k_3 c_S(t))}{v_0 + k_1(c_{s\max} - c_S(t))} - k_3 c_S(t)\frac{A_\mathrm{ST}}{A_\mathrm{A}}$	Mass balance on Control Volume 2
Equation S5	$\frac{\partial c}{\partial t} = D_t\frac{\partial^2 c}{\partial y^2}$	Diffusion in the tubule
	$c(0,t) = k_4 c_S(t),\ c(L_t,t) = 0$	Boundary conditions at the entrance and at the end of the tubule
	$\frac{\partial c}{\partial t}(L_t,t) = 0$	Alternative condition at the end of the tubule